

## Short communication

## The effects of temperature and different precursors in the synthesis of nano spinel in KCl molten salt

Y. Safaei-Naeini<sup>a</sup>, M. Aminzare<sup>a,b,\*</sup>, F. Golestani-Fard<sup>a,c</sup><sup>a</sup> School of Metallurgy and Materials Engineering, Iran University of Science and Technology, Tehran, Iran<sup>b</sup> Materials and Energy Research Center (Merc), Karaj, Iran<sup>c</sup> Center of Excellence for Advanced Materials and Processing (CEAMP), Iran University of Science and Technology<sup>1</sup>, Tehran, Iran

Received 10 May 2011; received in revised form 31 July 2011; accepted 4 August 2011

Available online 11th August 2011

## Abstract

Nano-particles of  $\text{MgAl}_2\text{O}_4$  were successfully synthesized at  $850^\circ\text{C}$  using the molten-salt method, and the effects of processing parameters, such as the amount and type of precursor and temperature on the crystallization of  $\text{MgAl}_2\text{O}_4$ , were investigated. Spinel nano powders were synthesized by heating stoichiometric compositions of different  $\text{MgO}$ - and  $\text{Al}_2\text{O}_3$ -bearing precursors in potassium chlorides (KCl). The phase formation, morphology and purity of these powders were characterized via X-ray diffraction (XRD), scanning electron microscopy (SEM) and X-ray fluorescence (XRF), respectively. The results demonstrated that the formation of  $\text{MgAl}_2\text{O}_4$  spinel could be initiated at  $850^\circ\text{C}$  and that, after the temperature was increased to  $1000^\circ\text{C}$ , the amounts of  $\text{MgAl}_2\text{O}_4$  in the resultant powders increased with a concomitant decrease of  $\text{MgO}$  and  $\text{Al}_2\text{O}_3$ . Furthermore, the synthesized  $\text{MgAl}_2\text{O}_4$  grains retained the size and morphology of the  $\text{Al}_2\text{O}_3$  powders, which indicated that a template formation mechanism dominated the formation of  $\text{MgAl}_2\text{O}_4$  by molten-salt synthesis.

© 2011 Elsevier Ltd and Techna Group S.r.l. All rights reserved.

Keywords: Synthesis; Nano spinel; Molten salt

## 1. Introduction

Molten-salt synthesis (MSS) is appreciated as a straight forward method for the preparation of ceramic powders with whisker-like, needle-like or plate-like morphologies [1–4]. This synthesis technique is a well-established process of forming a target compound in a flux with a low melting point [5–7]. MSS offers a significant reduction in the formation temperature compared to a conventional solid-state reaction. It also provides noticeable control of the particle size and morphology of the resulting powders [8,9].

The molten-salt synthesis method is based on the use of salts with low melting points that are water soluble, such as alkali chlorides and sulfates, for the synthesis of ceramics. This method avoids leaving high levels of impurities in the final

product powder [5,7,10]. Numerical studies of the MSS technique are available in the literature that involve the preparation of ferroelectrics, dielectrics, piezoelectrics, pyroelectrics, spinel and mullite using various alkali salts [11–13]. The selection of an appropriate salt significantly influences the ability of the reaction to produce desirable powder morphologies and characteristics. The selection of the salt is highly dependent on two criteria: the melting point of the salt should be low and appropriate for the synthesis of the required phase, and the salt should exhibit sufficient aqueous solubility to be easily eliminated by a simple washing after the synthesis [10].

As previously reported [10,14], the solubility of the reactants in the molten salt plays an important role in MSS processes. The solubilities affect both the reaction rate and the morphology of the synthesized grains. If both of the reactants are soluble in the molten salt, then the product phase can be readily synthesized via precipitation from the salt that contains the dissolved reactants (“dissolution–precipitation” mechanism) [10,14,15]. In this case, the morphologies of the product grains will be generally different from those of the reactants. However, if one reactant is significantly more soluble than another reactant, the more-soluble reactant will dissolve into

\* Corresponding author at: School of Metallurgy and Materials Engineering, Iran University of Science and Technology, Tehran, Iran.  
Tel.: +98 912 5636521.

E-mail addresses: [masoudaminzare@gmail.com](mailto:masoudaminzare@gmail.com),  
[masoudaminzare@yahoo.com](mailto:masoudaminzare@yahoo.com) (M. Aminzare).

<sup>1</sup> Website: [rrg.iust.ac.ir](http://rrg.iust.ac.ir).

Table 1  
Composition and firing conditions of all powder mixtures.

| Sample code | Starting materials <sup>a</sup> | Temperature (°C) | Time (h) | Salt/oxide weight ratio |
|-------------|---------------------------------|------------------|----------|-------------------------|
| S1          | A–M–KCl                         | 850              | 3        | 3/1                     |
| S2          | A–NM–KCl                        | 850              | 3        | 3/1                     |
| S3          | NA–M–KCl                        | 850              | 3        | 3/1                     |
| S4          | NA–NM–KCl                       | 850              | 3        | 3/1                     |
| S5          | NB–M–KCl                        | 850              | 3        | 3/1                     |
| S6          | NB–NM–KCl                       | 850              | 3        | 3/1                     |
| S7          | A–M–KCl                         | 1000             | 3        | 3/1                     |
| S8          | A–NM–KCl                        | 1000             | 3        | 3/1                     |
| S9          | NA–M–KCl                        | 1000             | 3        | 3/1                     |
| S10         | NA–NM–KCl                       | 1000             | 3        | 3/1                     |
| S11         | NB–M–KCl                        | 1000             | 3        | 3/1                     |
| S12         | NB–NM–KCl                       | 1000             | 3        | 3/1                     |

<sup>a</sup> A = alumina, M = magnesia, NA = nano alumina, NB = nano boehmite, NM = nano magnesia.

the salt first and then diffuse onto surfaces of the less-soluble reactant, where it reacts in situ to form the product phase. In this case, the size and morphology of the synthesized grains would, to a large extent, be similar to the reactant size and morphology produced by the less-soluble reactant (“template formation” mechanism) [10,14,15].

Spinel consist of a group of cubic double oxides that includes magnesium aluminate (MA) spinel, which finds widespread use in the refractory materials industry because of its high refraction, low thermal expansion, strong hydration resistance, good mechanical strength, and remarkable chemical resistance [16–20]. Spinel (MA) can be synthesized in a number of ways [21–25]. Commercially, the most popular method is conventional oxide mixing, which involves a solid-state reaction between MgO- and Al<sub>2</sub>O<sub>3</sub>-bearing precursors such as oxides, hydroxides, and carbonates [16–18]. Like many solid-state reactions, it takes place via slow counter-diffusion of ions. Other synthesis techniques, such as freeze-drying, sol–gel processing of metal alkoxides and co-precipitation, have also been applied for the synthesis of MA spinel. However, these routes suffer from complexity, are environmentally unfriendly, lack reproducibility and involve expensive precursors [10,14,15].

In the present paper, the molten-salt synthesis method was used to prepare nano-crystalline MgAl<sub>2</sub>O<sub>4</sub>. Additionally, the effect of different precursors on the synthesis temperature of nano-crystalline MgAl<sub>2</sub>O<sub>4</sub> was studied.

## 2. Experimental procedure

Five different MgO- and Al<sub>2</sub>O<sub>3</sub>-bearing precursors, including Al<sub>2</sub>O<sub>3</sub> (Merck, Germany,  $D_{50}$  = 3  $\mu$ m), MgO (Merck, Germany,  $D_{50}$  = 3  $\mu$ m), nano boehmite (Sasol, Germany, assay 99.8%,  $D_{50}$  = 40 nm), nano magnesia (Ionic Liquid Technologies, assay 99.9%,  $D_{50}$  = 35 nm), and nano alumina (Ionic Liquid Technologies, assay 99.9%,  $D_{50}$  = 40 nm) were used as primary raw materials in addition to KCl (Merck, assay 99%), which was employed as the molten salt in this work.

For sample preparation, an equimolar composition of different raw materials, such as the MgO- and Al<sub>2</sub>O<sub>3</sub>-bearing

precursors, were separately dispersed in doubly deionized water using a magnetic stirrer and an ultrasonic probe. Then, the MgO-bearing precursor dispersion was added to the obtained dispersed Al<sub>2</sub>O<sub>3</sub>-bearing precursor suspension, and the mixtures were stirred and heated to remove the media dispersion. The mixtures were fully dried at 120 °C for 10 h. The dried and pulverized powder was finally mixed with KCl at a salt-to-oxide weight ratio of 3:1. The mixtures were heated in an alumina crucible and covered with an alumina lid for 3 h at a temperature between 850 and 1000 °C with a 3 °C/min heating rate. After cooling to room temperature, the solidified mass was washed and filtered in hot doubly deionized water several times to remove the salts. The obtained powder was then dried at 120 °C for 10 h. The composition and firing conditions of all the powdered mixtures are shown in Table 1. The crystalline phase and morphology of the powders were examined by X-ray diffraction (XRD, Philips pw3710) and scanning electron microscopy (SEM, Tescan Vega II), respectively. To elucidate the different reaction mechanisms in the synthesis of MA by the molten-salt method, differential scanning calorimetry (DSC) and thermogravimetric analysis (TGA) were performed at temperatures up to 1000 °C at a heating rate of 10 °C/min in air. The impurity levels of K and Cl that originated from the utilized salt were detected by X-ray fluorescence (XRF, Bruker AXS, Karlsruhe, Germany, SRS 3400) spectrometry.

## 3. Results and discussion

DSC/TGA was performed to determine the proper reaction temperature range as well as the reaction order in the molten-salt method. Fig. 1, for instance, shows DSC/TGA curves of a nano boehmite–magnesia–KCl mixture. The DSC curve exhibits two endothermic peaks, which are associated with a slow weight loss (10%) in the TGA curve from 200 to 350 °C. This weight loss is attributed to dehydration of the precursors and the decomposition of nano boehmite. The small exothermic peaks at approximately 400 °C are related to the transformation of boehmite to  $\gamma$ -alumina. Furthermore, the weight loss at temperatures just above 800 °C is attributed to the evaporation of KCl. This salt is known to melt at 770 °C and to begin to

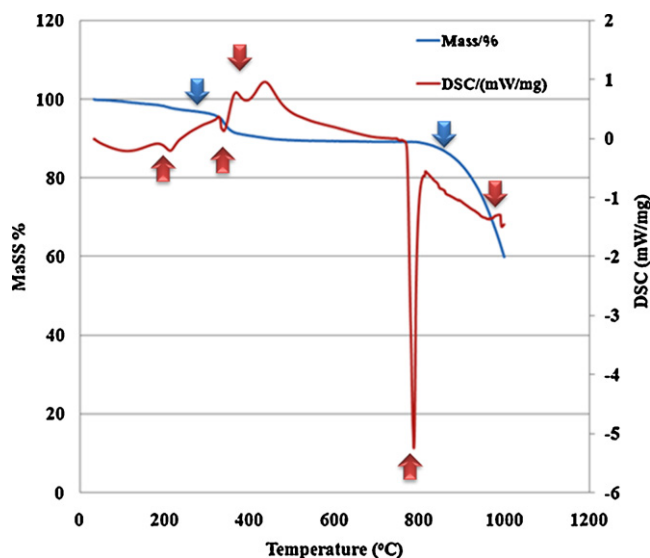


Fig. 1. DSC–TGA curve of a NB–M–KCl mixture heated to 1000 °C at a rate of 10 °C/min.

evaporate at approximately 800 °C [10,12,14]. The endothermic peaks at 780 °C correlate to the melting point of KCl salt, and the small exothermic peaks at 800–900 °C are interpreted as the formation of the spinel phase. Because the formation of spinel at approximately 900 °C is accompanied by severe evaporation of the salt, the peak intensity is rather low. In

addition, the low oxide-to-salt ratio (1:3) in the present batch results in a rather low-intensity peak in the DTA/TG pattern (Fig. 1).

Fig. 2(a) and (b) shows XRD patterns of the S1–S6 and S7–S12 samples, respectively, after they were heated under the conditions described in Table 1. As evident in the figures, the treatment of S1 and S2 samples at 850 °C for 3 h did not result in the formation of spinel peaks in the XRD patterns of these samples. After the specimens were heated for 3 h at 1000 °C (S7–S8 samples), the gradual formation of spinel peaks was observed; however,  $\text{Al}_2\text{O}_3$  and MgO peaks were still present. In the S3 and S4 samples, the spinel peaks began to appear after 3 h at 850 °C. The spinel peak intensities increased when the temperature of samples S9–S10 was increased to 1000 °C, whereas the  $\text{Al}_2\text{O}_3$  and MgO peaks disappeared. In samples S5 and S6, only a single-phase spinel was detected, and other  $\text{Al}_2\text{O}_3$  and MgO peaks disappeared after 3 h at 850 °C. As the temperature of samples S11–S12 was increased to 1000 °C, the spinel peak intensity increased significantly. Therefore, single-phase  $\text{MgAl}_2\text{O}_4$  could be prepared after 3 h at 850 °C in samples S5–S6. This temperature is at least 500 °C lower than that required for the conventional mixed-oxide synthesis method [16–18]. The decreased synthesis temperature was attributed to a more homogeneous mixing and a more rapid diffusion of species such as  $\text{Mg}^{2+}$  and  $\text{O}^{2-}$  in the MSS liquid/solid system than in the CMOS solid–solid system. Furthermore, the  $\gamma$ -alumina formed in situ is highly reactive, which

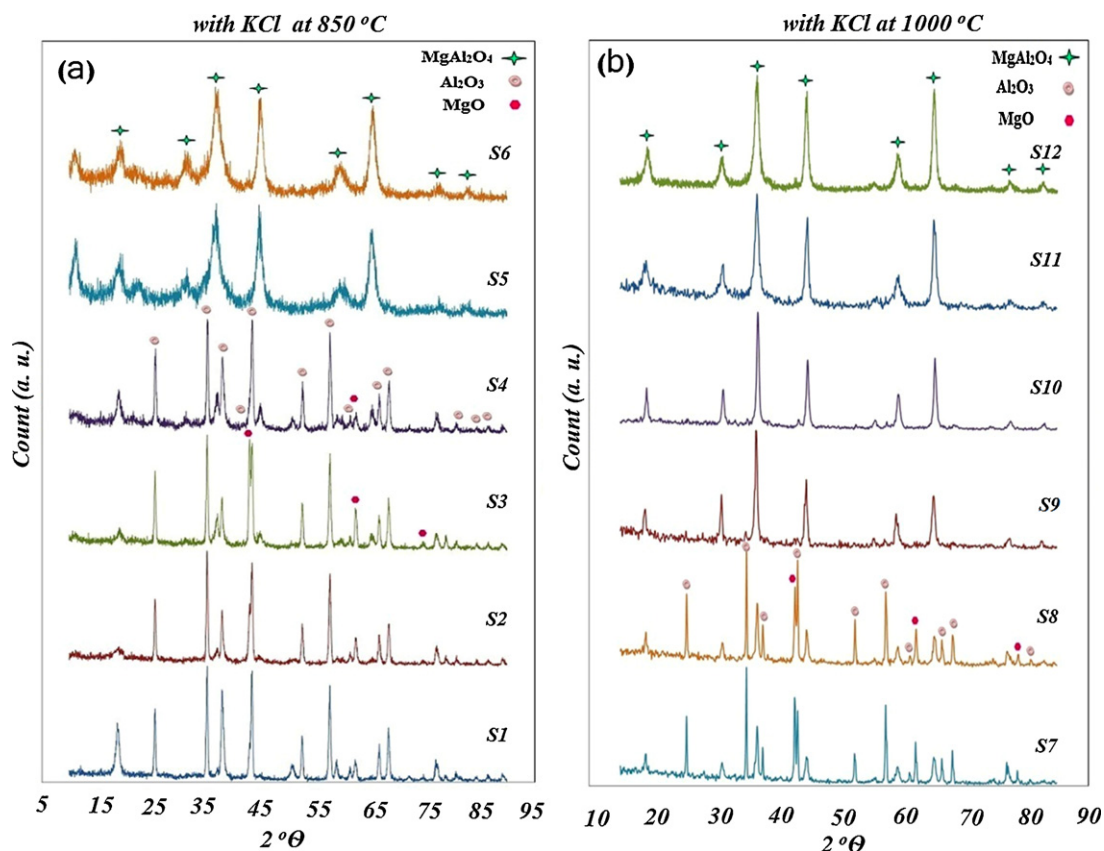


Fig. 2. XRD patterns of S1–S6 and S7–S12 samples heated at different temperatures: (a) 850 °C and (b) 1000 °C.



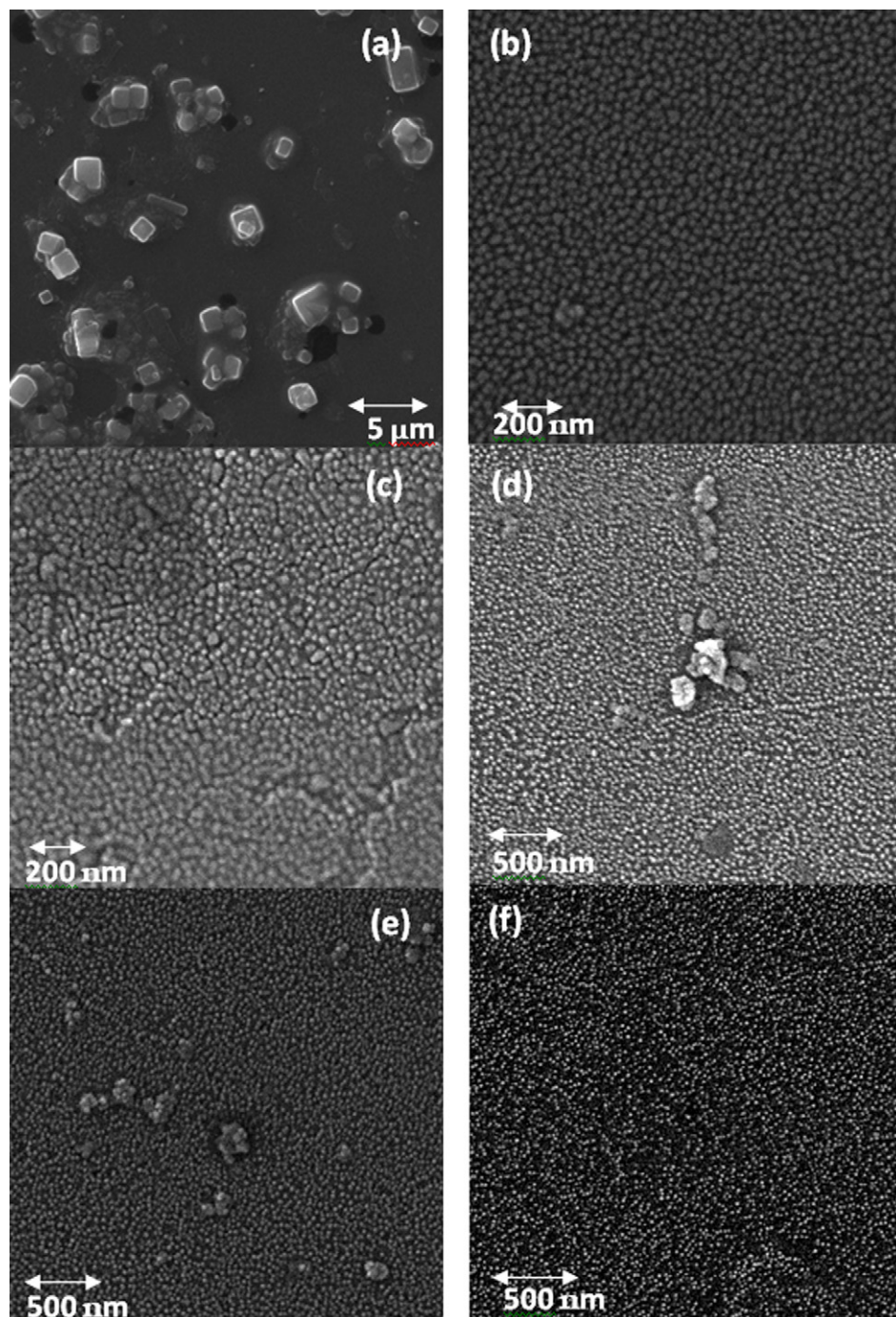


Fig. 3. SEM micrograph of the precursors and synthesized  $\text{MgAl}_2\text{O}_4$  powders: (a) magnesia, (b)  $\gamma\text{-Al}_2\text{O}_3$  formed from boehmite decomposition, (c) S9, (d) S5, (e) S12, (f) S6.

promotes its reactions with MgO and further lowers the  $\text{MgAl}_2\text{O}_4$  synthesis temperature relative to the previously reported temperature for the molten-salt synthesis of MA. As previously reported by other researchers [10,14–16], the formation of different phases depends on variable parameters such as temperature, time, and the amount and type of the precursors; i.e., the formation rate depends on the rate of migration of the magnesium ions and their diffusion rate into  $\text{Al}_2\text{O}_3$  particles in KCl media. For example, the use of nano-sized precursors can result in a significant decrease in the

migration distance and, therefore, can enhance the spinel formation. The phase content of a batch therefore depends on the precursor's size and the reaction conditions. In addition, the synthesis temperature used for the present route was similar to that used for “wet chemical synthesis” methods such as sol–gel and co-precipitation, but much less expensive and more environmentally friendly raw materials were used [21–25].

Table 2 shows the XRF analysis results of the MA powders synthesized in KCl and reveals that only minor salt components remained in the synthesized MA powders after washing. The

Table 2

Salt components remaining in the MA powders synthesized in KCl (wt%).

| Sample no. | MA formation temperature (°C) | Impurity levels (wt)% |                  |
|------------|-------------------------------|-----------------------|------------------|
|            |                               | Cl                    | K <sub>2</sub> O |
| S5         | 850                           | 0.12                  | 0.09             |
| S6         | 850                           | 0.09                  | 0.10             |
| S9         | 1000                          | 0.13                  | 0.12             |
| S10        | 1000                          | 0.11                  | 0.09             |
| S11        | 1000                          | 0.10                  | 0.07             |
| S12        | 1000                          | 0.08                  | 0.10             |

main objective of this table is to illustrate the feasibility of the molten-salt method for the synthesis of pure ceramic powders.

The morphologies of the dispersed magnesia and  $\gamma$ -alumina, which were obtained from the decomposition of primary boehmite, and that of the synthesized  $\text{MgAl}_2\text{O}_4$  nano powders are shown in Fig. 3. Nano  $\text{MgAl}_2\text{O}_4$  particles of uniform size and shape were obtained. The morphology of the  $\text{MgAl}_2\text{O}_4$  nano particles (spherical) was similar to that of the  $\gamma$ -alumina powders, which indicates that template growth plays an important role in molten-salt synthesis of  $\text{MgAl}_2\text{O}_4$  spinel [10,14,15].

#### 4. Conclusion

The introduction of the molten-salt medium into the reaction process allowed the synthesis of  $\text{MgAl}_2\text{O}_4$  nano-particles at much lower temperatures than those used in the conventional mixed-oxide synthesis (CMOS). Well-crystallized  $\text{MgAl}_2\text{O}_4$  nano-particles were easily prepared at 850 °C by the molten-salt method within a short holding time of 3 h using KCl as the molten-salt medium with a 3:1 weight ratio between the salt and different  $\text{MgAl}_2\text{O}_4$  precursors. The size and shape of the synthesized  $\text{MgAl}_2\text{O}_4$  grains were observed to be remarkably similar in size and morphology to the  $\text{AlOOH}$  powder, which indicates that a template formation mechanism has dominated the formation of  $\text{MgAl}_2\text{O}_4$  by the molten-salt synthesis process.

#### References

- [1] K. Chen, X. Zhang, Synthesis of calcium copper titanate ceramics via the molten salt method, *Ceram. Int.* 36 (2010) 1523–1527.
- [2] Z. Li-Hui, H. Qing-Wei, Morphology control of  $\alpha$ - $\text{Al}_2\text{O}_3$  platelets by molten salt, *Ceram. Int.* 37 (2011) 249–255.
- [3] N. Tawichai, W. Sittiyot, S. Eitssayeam, K. Pengpat, T. Tunkasiri, G. Rujijanagul, Preparation and dielectric properties of barium iron niobate by molten-salt synthesis, *Ceram. Int.* (2011), doi:10.1016/j.ceramint.2011.04.064, in press.
- [4] Z.Y. Zhan, C.Y. Xu, L. Zhen, W.S. Wang, W.Z. Shao, Large-scale synthesis of single-crystalline  $\text{KNb}_3\text{O}_8$  nano belts via a simple molten salt method, *Ceram. Int.* 36 (2010) 679–682.
- [5] Y. Liu, W. Yang, Z. Dai, H. Chen, X. Yang, D. Hou, Improved molten salt synthesis (MSS) for  $\text{SnO}_2$  nanorods and nano twins, *Mater. Chem. Phys.* 112 (2008) 381–386.
- [6] Z. Cai, X. Xing, L. Li, Y. Xu, Molten salt synthesis of lead lanthanum zirconate titanate ceramic powders, *J. Alloy Compd.* 454 (2008) 466–470.
- [7] Z. Li, S. Zhang, W.E. Lee, Molten salt synthesis of  $\text{LaAlO}_3$  powder at low temperatures, *J. Eur. Ceram. Soc.* 27 (2007) 3201–3205.
- [8] Y. Liu, J. Ma, Z. Liu, C. Dai, Z. Song, Y. Sun, J. Fang, J. Zhao, Low-temperature synthesis of  $\text{BiVO}_4$  crystallites in molten salt medium and their UV–vis absorption, *Ceram. Int.* 36 (2010) 2073–2077.
- [9] Z. Liu, J. Ma, Y. Sun, Z. Song, J. Fang, Y. Liu, C. Gao, J. Zhao, molten salt synthesis of  $\text{YAlO}_3$  powders assisted by an electrochemical process, *Ceram. Int.* 36 (2010) 2003–2006.
- [10] S. Zhang, Low temperature synthesis of complex refractory oxide powders from molten salts, *J. Pak. Mater. Soc.* 1 (2007) 49–53.
- [11] A. Baral, K.B.R. Varma, Low temperature molten-salt synthesis of nanocrystalline cubic  $\text{Sr}_2\text{SbMnO}_6$ , *J. Solid State Chem.* 182 (2009) 3282–3288.
- [12] H.-L. Li, Z.-N. Du, G.-L. Wang, Y.-C. Zhang, Low temperature molten salt synthesis of  $\text{SrTiO}_3$  submicron crystallites and nanocrystals in the eutectic  $\text{NaCl}$ – $\text{KCl}$ , *Mater. Lett.* 64 (2010) 431–434.
- [13] Z. Yang, Y. Chang, H. Li, Piezoelectric and dielectric properties of PZT–PZN–PMS ceramics prepared by molten salt synthesis method, *Mater. Res. Bull.* 40 (2005) 2110–2119.
- [14] W. Zhang, D.D. Jayaseelan, G. Bhattacharya, W.E. Lee, Molten salt synthesis of magnesium aluminate ( $\text{MgAl}_2\text{O}_4$ ) spinel powder, *J. Am. Ceram. Soc.* 89 (2006) 1724–1726.
- [15] D.D. Jayaseelan, S. Zhang, S. Hashimoto, W.E. Lee, Template formation of magnesium aluminate ( $\text{MgAl}_2\text{O}_4$ ) spinel microplatelets in molten salt, *J. Eur. Ceram. Soc.* 27 (2007) 4745–4749.
- [16] I. Ganesh, G.J. Reddy, G. Sundararajan, S.M. Olhero, P.M.C. Torres, J.M.F. Ferreira, Influence of processing route on microstructure and mechanical properties of  $\text{MgAl}_2\text{O}_4$  spinel, *Ceram. Int.* 36 (2010) 473–482.
- [17] I. Ganesh, Fabrication of magnesium aluminate ( $\text{MgAl}_2\text{O}_4$ ) spinel foams, *Ceram. Int.* 37 (2011) 2237–2245.
- [18] R. Naghizadeh, H.R. Rezaie, F. Golestani-Fard, Effect of  $\text{TiO}_2$  on phase evolution and microstructure of  $\text{MgAl}_2\text{O}_4$  spinel in different atmospheres, *Ceram. Int.* 37 (2011) 349–354.
- [19] H.S. Tripathi, A. Ghosh, Spinelisation and properties of  $\text{Al}_2\text{O}_3$ – $\text{MgAl}_2\text{O}_4$ –C refractory effect of  $\text{MgO}$  and  $\text{Al}_2\text{O}_3$  reactants, *Ceram. Int.* 36 (2010) 1189–1192.
- [20] A. Banerjee, S. Das, S. Misra, S. Mukhopadhyay, Structural analysis on spinel ( $\text{MgAl}_2\text{O}_4$ ) for application in spinel-bonded castables, *Ceram. Int.* 35 (2009) 381–390.
- [21] M.K. Naskar, M. Chatterjee, Magnesium aluminate ( $\text{MgAl}_2\text{O}_4$ ) spinel powders from water-based sols, *J. Am. Ceram. Soc.* 88 (2005) 38–44.
- [22] M.F. Zawrah, H. Hamaad, S. Meky, Synthesis and characterization of nano  $\text{MgAl}_2\text{O}_4$  spinel by the co-precipitated method, *Ceram. Int.* 33 (2007) 969–978.
- [23] R. Ianoş, R. Lazău, Combustion synthesis, characterization and sintering behavior of magnesium aluminate ( $\text{MgAl}_2\text{O}_4$ ) powders, *Mater. Chem. Phys.* 115 (2009) 645–648.
- [24] I. Ganesh, R. Johnson, G.V.N. Rao, Y.R. Mahajan, S.S. Madavendra, B.M. Reddy, Microwave-assisted combustion synthesis of nanocrystalline  $\text{MgAl}_2\text{O}_4$  spinel powder, *Ceram. Int.* 31 (2005) 67–74.
- [25] A. Saberi, F. Golestani-Fard, M. Willert-Porada, Z. Negahdari, C. Liebscher, B. Gossler, A novel approach to synthesis of nanosize  $\text{MgAl}_2\text{O}_4$  spinel powder through sol–gel citrate technique and subsequent heat treatment, *Ceram. Int.* 35 (2009) 933–937.